Open access • Journal Article • DOI:10.1088/0031-9155/41/1/003

Imaging laser heated subsurface chromophores in biological materials: Determination of lateral physical dimensions — Source link

Thomas E. Milner, Thomas E. Milner, Dennis M. Goodman, B. Samuel Tanenbaum ...+4 more authors

Institutions: Harvey Mudd College, University of California, Irvine, Lawrence Livermore National Laboratory, Norwegian Institute of Technology

Published on: 01 Jan 1996 - Physics in Medicine and Biology (IOP Publishing)

Topics: Laser and Attenuation coefficient

Title
Imaging laser heated subsurface chromophores in biological materials: determination of lateral physical dimensions.

Journal
Physics in medicine and biology, 41(1)

ISSN
0031-9155

Authors
Milner, TE
Goodman, DM
Tanenbaum, BS
et al.

Publication Date
1996

DOI
10.1088/0031-9155/41/1/003

Phys. Med. Biol. **41** (1996) 31–44. Printed in the UK

Imaging laser heated subsurface chromophores in biological materials: determination of lateral physical dimensions

Thomas E Milner†‡, Dennis M Goodman§, B Samuel Tanenbaum‖, Bahman Anvari†‖, Lars O Svaasand¶ and J Stuart Nelson†

† University of California, Beckman Laser Institute and Mecial Clinic, Irvine, CA, USA
‡ Harvey Mudd College, Department of Physics, Claremont, CA, USA
§ Lawrence Livermore National Laboratory, University of California, Livermore, CA, USA
‖ Harvey Mudd College, Department of Engineering, Claremont, CA, USA
¶ Division of Physical Electronics, University of Trondheim, Norwegian Institute of Technology, Trondheim, Norway

Received 9 June 1995, in final form 12 September 1995

Abstract. We describe a non-contact method using infrared radiometry to determine lateral physical dimensions of laser heated subsurface chromophores in biological materials. An imaging equation is derived that relates measured radiometric temperature change to the reduced two-dimensional temperature increase of laser heated chromophores. From measured images of radiometric temperature change, the lateral physical dimensions of chromophores positioned in an *in vitro* model of human skin are determined by deconvolution of the derived imaging equation using a non-negative constrained conjugate gradient algorithm. Conditions for optimum spatial resolution are found by analysis of a derived radiometric transfer function and correspond to superficial chromophores and/or weak infrared absorption in a laser irradiated biological material. Analysis indicates that if the infrared attenuation coefficient is sufficiently small (i.e., less than 10 mm^{-1}), infrared radiometry in combination with a deconvolution algorithm allows estimation of lateral physical dimensions of laser heated subsurface chromophores in human skin.

1. Introduction

Successful laser treatment of selected dermatoses requires controlled photothermal destruction of discrete subsurface chromophores in human skin. Because physical dimensions of targeted subsurface chromophores determine thermal relaxation time (τ_r), proper selection of laser pulse duration (t_p) is critical for successful treatment. For example, selective photothermolysis of port wine stain (PWS) blood vessels in human skin (Anderson and Parish 1983) requires matching laser pulse duration to thermal relaxation time of targeted vessels (i.e., $t_p \sim \tau_r$) (Kimel *et al* 1993). In this case, τ_r is proportional to squared diameter, and thus proper selection of t_p requires knowledge of the lateral physical dimensions of the targeted blood vessels.

A number of investigators have reported application of pulsed photothermal radiometry using a single-element infrared detector to determine various optical, thermal, and structural properties of semiconductor (Tam 1987) and biological materials (Prahl *et al* 1992, Vitkin *et al* 1995, Milner *et al* 1995). We describe a non-contact method using infrared imaging radiometry to determine lateral physical dimensions of subsurface laser heated

0031-9155/96/010031+14$19.50

chromophores in an *in vitro* biological material. In response to a diagnostic laser pulse, the true radiometric temperature increase is measured by a fast infrared focal plane array (IR FPA) camera. Due to inherent limitations of the camera (i.e., size of the collection aperture, lens aberrations, finite number and size of discrete detector elements) and thermal diffusion in the irradiated biological material, lateral physical dimensions of laser heated chromophores can not be directly measured in any one radiometric temperature image. In early images when blurring due to heat diffusion is least, the signal-to-noise ratio (SNR) of the true radiometric temperature increase is reduced when chromophores are imbedded deep within the material. Although SNR may be higher in later images as heat moves to the surface, lateral resolution decreases as thermal diffusion and blurring increase. To estimate lateral physical dimensions of laser heated subsurface chromophores in biological materials, we introduce the reduced two-dimensional temperature increase $[\Delta T^{2D}(x, y, t_0)]$. From a measured image of radiometric temperature change, $\Delta T^{2D}(x, y, t_0)$ is determined by deconvolution of the derived imaging equation; lateral physical dimensions of subsurface chromophores are readily deduced from $\Delta T^{2D}(x, y, t_0)$.

First, we derive the imaging equation and discuss use of a deconvolution algorithm to determine the reduced two-dimensional temperature increase $(\Delta T^{2D}(x, y, t_0))$ of laser heated subsurface chromophores from a measured image of the radiometric temperature change $(\Delta M(x, y, t_0))$. Second, experiments are described that measure the radiometric temperature change following pulsed laser irradiation of chromophores positioned at various depths in an *in vitro* biological material. Third, the reduced two-dimensional temperature increase of subsurface chromophores is computed by deconvolution of the derived imaging equation using selected measured images of radiometric temperature change $(\Delta M(x, y, t_0))$ and a non-negative constrained conjugate gradient algorithm. Following discussion of experimental results, we derive an analytic expression for a radiometric transfer function and examine effects of chromophore depth (z_0) and infrared absorption coefficient (μ_{ir}) on spatial resolution.

2. Theory

We derive an imaging equation that relates the reduced two-dimensional temperature increase $(\Delta T^{2D}(x, y, t_0))$ of laser heated subsurface chromophores in a biological material to a measured image of radiometric temperature change $(\Delta M(x, y, t_0))$. Our analysis includes effects of heat diffusion and inherent limitations of the IR FPA camera used to measure $\Delta M(x, y, t_0)$. Because the imaging equation cannot be solved uniquely for $\Delta T^{2D}(x, y, t_0)$, deconvolution of an image of measured radiometric temperature change $(\Delta M(x, y, t_0))$ is necessary. Given the biophysical properties of a laser irradiated material and specifications of the IR FPA camera, application of a numerical algorithm allows deconvolution of the derived imaging equation and thus estimation of lateral physical dimensions of subsurface chromophores.

2.1. The imaging equation

For the purpose of computing the thermal component of the imaging equation point spread function, we assume a δ pulse of energy, $q[J]$, is released within a semi-infinite medium (depth $z = \zeta_0$, time $t = 0$) representing a biological material (figure 1) and seek a Green's function solution, ΔT_δ, to the bioheat equation (van Gemert *et al* 1991),

$$\nabla^2(\Delta T_\delta) - (1/\chi)\partial(\Delta T_\delta)/\partial t - (Q/\chi)\Delta T_\delta = -(q/\kappa)\delta(t)\delta(x)\delta(y)\delta(z - \zeta_0). \tag{1}$$

In (1) Q (s^{-1}) represents the volume fraction of blood perfused tissue per unit time; κ (W m^{-1} K^{-1}) and χ (m^2 s^{-1}) are, respectively, thermal conductivity and diffusivity of the laser irradiated biological material which we assume are homogeneous. Additionally, we assume a Robin type boundary condition,

$$\kappa[\partial(\Delta T_\delta)/\partial z]|_{z=0} = h\Delta T_\delta|_{z=0} \tag{2}$$

in which the heat loss coefficient h (W m^{-2} K^{-1}), represents combined radiative and/or convective thermal energy losses at the air–material interface.

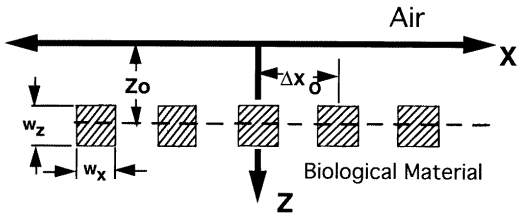

Figure 1. The geometry assumed in derivation of the imaging equation and radiometric transfer function.

Solution of the bioheat equation ($\Delta T_\delta(\xi, \eta, \zeta, t)$) represents the increase in temperature above ambient values at position (ξ, η, ζ) and time (t) in response to a δ pulse of energy released at position $(0, 0, \zeta_0)$ and time $t = 0$.

$$\Delta T_\delta(\xi, \eta, \zeta, t) = [q\mathrm{e}^{-Qt}/(4\pi t)^{3/2}\kappa\chi^{1/2}]\mathrm{e}^{-(\xi^2+\eta^2)/4\chi t}\{\mathrm{e}^{-(\zeta-\zeta_0)^2/4\chi t} + \mathrm{e}^{-(\zeta+\zeta_0)^2/4\chi t} \times[1 - (h/\kappa)\sqrt{4\pi\chi t}\,\mathrm{erfcx}(u)]\} \tag{3}$$

where

$$u = (\zeta + \zeta_0)/2\sqrt{\chi t} + (h/\kappa)\sqrt{\chi t}$$

and $\mathrm{erfcx}(u) = \exp(u^2)\mathrm{erfc}(u)$, where $\mathrm{erfc}(\cdot)$ is the complementary error function $[1-\mathrm{erf}(\cdot)]$.

Infrared emission from laser heated subsurface chromophores is scattered and absorbed prior to exiting the material. We assume reduced lateral resolution due to scattering of infrared radiation (Gaussian parameter $\sigma_s(m)$), and an exponential loss (absorption coefficient μ_{ir} (m^{-1})), and write the relative increase in infrared emission at position $r = (x^2 + y^2)^{1/2}$ on the surface due to an infinitesimal volume of excess thermal energy (with unit temperature difference above the background level) located at position (ξ, η, ζ),

$$\mu_{ir}\,\mathrm{e}^{-\mu_{ir}\zeta}(1/2\pi\sigma_s^2)\mathrm{e}^{-[(x-\xi)^2+(y-\eta)^2]/2\sigma_s^2}. \tag{4}$$

The Gaussian parameter, σ_s, accounts for lateral blur due to scattering of infrared radiation emitted from the sample. Although the actual functional form of the blur is probably not Gaussian, the approximation in (4) is well founded when one considers scattering phase functions frequently used in light fluence computations in biological tissues (Ishimaru 1978). By integrating the excess thermal energy over the entire material volume and assuming that the blood perfusion relaxation time is much longer than the duration of measurement ($(1/Q) \gg t$), we find the three-dimensional thermal point spread function (K_T),

$$K_T \propto \frac{\mu_{ir}}{2\pi\sigma_s^2}\int_\xi\int_\eta\int_\zeta \mathrm{e}^{-\mu_{ir}\zeta}\,\mathrm{e}^{-[(x-\xi)^2+(y-\eta)^2]/2\sigma_s^2}\Delta T_\delta(\xi, \eta, \zeta, t)\,\mathrm{d}\xi\,\mathrm{d}\eta\,\mathrm{d}\zeta. \tag{5}$$

Substituting the thermal response of tissue ($\Delta T_\delta(\xi, \eta, \zeta, t)$, (3)) to a δ pulse of energy, q (depth $z = \zeta_0$), into equation (5), gives

$$K_T \propto [q\mu_{ir}/\rho_t C_t(2\sigma_s^2 + 4\chi t)2\pi]\mathrm{e}^{-(x^2+y^2)/(2\sigma_s^2+4\chi t)}\mathrm{e}^{-\zeta_0^2/4\chi t}\{\mathrm{erfcx}(u_+) + \mathrm{erfcx}(u_-) - [2h/(h - \kappa\mu_{ir})][\mathrm{erfcx}(u_+) - \mathrm{erfcx}(u_1)]\} \tag{6}$$

where

$$u_\pm = \mu_{ir}\sqrt{\chi t} \pm \zeta_0/2\sqrt{\chi t} \qquad u_1 = (h/\kappa)\sqrt{\chi t} + \zeta_0/2\sqrt{\chi t} \tag{7}$$

ρ_t and C_t are, respectively, the mass density (kg m^{-3}) and specific heat capacity (J kg^{-1} K^{-1}). Additionally, we have assumed that the infrared absorption coefficient (μ_{ir}) is independent of depth and constant over relevant temperature changes. Furthermore, the scattering parameter (σ_s) is assumed constant and characteristic of infrared emission from a given depth ($\sim 1/\mu_{ir}$). Since $q/(\rho_t C_t)$ represents the initial temperature increase at position $(0, 0, \zeta_0)$, K_T is written

$$K_T(x - \xi, y - \eta, t, \zeta_0) = K_r(x - \xi, y - \eta, t)K_z(t, \zeta_0) \tag{8}$$

and consists of two physically distinct terms ((9*a*) and (9*b*) below) that represent, respectively, heat diffusion along lateral (K_r) and longitudinal (K_z) axes,

$$K_r(x, y, t) = [1/\pi(2\sigma_s^2 + 4\chi t)]\mathrm{e}^{-(x^2+y^2)/(2\sigma_s^2+4\chi t)} \tag{9a}$$

$$K_z(t, \zeta_0) = (\mu_{ir}/2)\mathrm{e}^{-\zeta_0^2/4\chi t}\{\mathrm{erfcx}(u_+) + \mathrm{erfcx}(u_-) - \{2(h/\kappa)/[(h/\kappa) - \mu_{ir}]\}[\mathrm{erfcx}(u_+) - \mathrm{erfcx}(u_1)]\}. \tag{9b}$$

Determination of K_T allows computation of true radiometric temperature increase ($\Delta R(x, y, t)$) as a convolution integral ((10) below) in terms of the initial three-dimensional temperature increase ($\Delta T^{3D}(x, y, z, t = 0)$),

$$\Delta R(x, y, t) = \int_{\xi,}\int_{\eta,}\int_{\zeta} \mathrm{d}\xi\, \mathrm{d}\eta\, \mathrm{d}\zeta\, K_T(x - \xi, y - \eta, \zeta, t)\Delta T^{3D}(\xi, \eta, \zeta, t = 0). \tag{10}$$

The effect of lateral heat diffusion on the true radiometric temperature increase ($\Delta R(x, y, t)$) can be understood by writing (10) in terms of the reduced two-dimensional subsurface temperature increase ($\Delta T^{2D}(x, y, t_0)$, (12) below) and convolution operator $*$

$$\Delta R(x, y, t_0) = \int_{\xi,}\int_{\eta} \mathrm{d}\xi\, \mathrm{d}\eta K_r(x - \xi, y - \eta, t_0)\Delta T^{2D}(\xi, \eta, t_0) = K_r * \Delta T^{2D} \tag{11}$$

$$\Delta T^{2D}(x, y, t_0) = \int_{\zeta} K_z(t_0, \zeta)\Delta T^{3D}(x, y, \zeta, t = 0)\, \mathrm{d}\zeta. \tag{12}$$

The lateral distribution of the true radiometric temperature increase (i.e., the x, y dependence of $\Delta R(x, y, t)$) is given by a convolution integral of the thermal point spread function, K_r, and $\Delta T^{2D}(x, y, t_0)$. $\Delta T^{2D}(x, y, t_0)$ (12) represents the reduced two-dimensional radiometric temperature increase of laser heated chromophores without effects of lateral blurring or limitations of the IR FPA camera. The objective of the work presented here is determination of $\Delta T^{2D}(x, y, t_0)$ from a measured image of radiometric temperature change ($\Delta M(x, y, t_0)$).

Because the true radiometric temperature increase ($\Delta R(x, y, t)$) is not measured directly, a realistic model should include inherent limitations of the IR FPA camera (i.e., the size of the collection aperture, lens aberrations, and the finite number and size of discrete detector elements). Since an IR FPA camera is a linear imaging system of incoherent light, the measured radiometric temperature change ($\Delta M(x, y, t_0)$) of a laser irradiated biological

material can be written (Goodman 1968) as a convolution integral ((13) below) of the camera point spread function (K_C) and true radiometric temperature increase, $\Delta R(x', y', t)$.

$$\Delta M(x, y, t_0) = \int_{x',} \int_{y'} \mathrm{d}x' \, \mathrm{d}y' K_C(x - x', y - y') \Delta R(x', y', t_0) = K_C * \Delta R. \tag{13}$$

Since $\Delta R(x', y', t)$ is expressible as a convolution integral (11), we may write an expression ((14) below) for the imaging equation in terms of the two-dimensional thermal (K_r) and camera (K_C) point spread functions,

$$\Delta M(x, y, t_0) = \int_{\xi,} \int_{\eta} (K_c * K_r)(x - \xi, y - \eta, t_0) \Delta T^{2D}(\xi, \eta, t = 0) \, \mathrm{d}\xi \, \mathrm{d}\eta \tag{14a}$$

$$\Delta M = (K_c * K_r) * \Delta T^{2D}. \tag{14b}$$

As written, the imaging equation represents a *forward* problem in which the recorded time sequence of images of the radiometric temperature change ($\Delta M(x, y, t_0)$) may be computed from the reduced two-dimensional temperature ($\Delta T^{2D}(x, y, t_0)$) and known biophysical properties of the material. Our objective, however, is to determine the reduced two-dimensional temperature increase ($\Delta T^{2D}(x, y, t_0)$) immediately following pulsed laser irradiation in order to remove blurring effects due to thermal diffusion or inherent limitations of the IR FPA camera. Inasmuch as only a timed sequence of images of radiometric temperature ($\Delta M(x, y, t)$) is available as input data, determination of $\Delta T^{2D}(x, y, t_0)$ in the imaging equation constitutes a deconvolution problem.

2.2. The deconvolution problem

The imaging equation (14) can be viewed as a two-dimensional deconvolution problem in which the unknown ($\Delta T^{2D}(x, y, t_0)$, (12)) is the reduced two-dimensional temperature increase of laser heated subsurface chromophores without blurring effects due to lateral thermal diffusion or the IR FPA camera. The imaging equation can be approximated as a linear matrix problem in which $\Delta T^{2D}(x, y, t_0)$ and the point spread function ($K = K_c * K_r$) are represented by, respectively, vector and matrix quantities ((15) below); here, bold symbols are used to represent vector and/or matrix terms.

$$\Delta \boldsymbol{M} = \mathbf{K} \Delta \boldsymbol{T}^{2D}. \tag{15}$$

The discretized imaging equation (15) is ill posed and cannot be solved directly because some singular values of the matrix $\mathbf{K}$ are essentially zero (i.e., less than the noise level). To find a realistic solution to this equation, a regularization term ($\Lambda \Delta \boldsymbol{T}^{2D}$) is included and the L_2 or Euclidean norm, f, is minimized with respect to $\Delta \boldsymbol{T}^{2D}$,

$$f(\Delta \boldsymbol{T}^{2D}, \Lambda) = \left\| \begin{bmatrix} \mathbf{K} \\ \sqrt{\Lambda} \end{bmatrix} \Delta \boldsymbol{T}^{2D} - \begin{bmatrix} \Delta \boldsymbol{M} \\ \mathbf{0} \end{bmatrix} \right\|^2. \tag{16}$$

Here $\Delta \boldsymbol{M}$ is a vector with N^2 components representing measured radiometric temperature change at time t_0 by individual detector elements in an $N \times N$ IR FPA; $\mathbf{K}$ is an $N^2 \times N^2$ matrix representing the point spread function ($K = K_c * K_r$) of the imaging equation; and $\Delta \boldsymbol{T}^{2D}$ is a N^2-component vector containing the unknown reduced two-dimensional temperature increase of laser heated subsurface chromophores.

The ill posedness of the deconvolution problem originates in attenuation of higher-order spatial frequencies due to lateral thermal diffusion ((9*a*); K_r) and inherent limitations of the IR FPA camera ((14), K_c). A variety of methods exist for solving linear least-squares imaging problems; however, the large dimension of the deconvolution problem

make iterative methods particularly attractive. Inasmuch as iterative spatial domain methods allow treatment of nonlinear problems and minimize 'ringing' effects (i.e., numerical oscillation), they are usually preferred over frequency domain techniques. Spatial domain methods, however, require storage and inversion of a $N^2 \times N^2$ matrix and, therefore, cannot immediately be applied to solve the deconvolution problem. For example, when a 128×128 IR FPA is used, double-precision representation of the matrix $\mathbf{K}$ in the discretized imaging equation requires a storage capacity of greater than 2 GB. In contrast, frequency domain methods require less storage space and reduce the number of computations [$\approx (N \log N)^2$] by utilizing the fast Fourier transform (FFT). A spatial domain algorithm that implements successive iterations in the frequency domain has been developed (Goodman *et al* 1992) that significantly reduces computation time. The method is based on conjugate gradients and uses a bending line search (McCormick 1989) and an active set strategy for implementation of the non-negativity constraint (i.e., $\Delta T^{2D}(x, y, t_0) \geqslant 0$) to give a highly efficient algorithm for image processing problems.

3. Materials and methods

Experiments are described that record a time sequence of images of radiometric temperature change ($\Delta M(x, y, t)$) in response to pulsed laser irradiation of an *in vitro* collagen material that contains subsurface chromophores positioned at various depths. An efficient non-negative constrained conjugate gradient algorithm is used to deconvolve the imaging equation and thus estimate lateral physical dimensions of the chromophores.

In each experiment, a pulsed laser source was used to expose an *in vitro* collagen material containing subsurface chromophores. A three-element infrared lens ($f/2$, 50 mm focal length) imaged true radiometric temperature ($R(x, y, t)$) onto a 128×128 InSb IR FPA (AE-4128, Amber Engineering, Goleta, CA, USA). The *in vitro* collagen model was positioned approximately 190 mm from the infrared imaging lens, giving an image to object geometric magnification of 0.4. Efforts to increase spatial resolution by repositioning the lens resulted in unacceptable lens aberrations and large dark-field radiometric temperature variations due to vignetting. The IR FPA camera acquired 217 images of radiometric temperature per second and was externally triggered by a digital delay generator that was optically triggered by a fast silicon photoreceiver. The infrared signal collected by each detector element in the IR FPA was digitized with a 3.5 MHz 12 bit A/D converter, immediately stored in the computer's random access memory, and later downloaded to a magneto-optic disk storage device (figure 2). A bandpass infrared filter (3–5 μm) was positioned near the cold stop of the IR FPA to reduce background fluctuations and, hence, increase SNR,

$$\mathrm{SNR} = \overline{\Delta M}/\mathrm{NE}\Delta T \tag{17}$$

where $\overline{\Delta M}$ is defined as the mean measured radiometric temperature change due to laser heated subsurface chromophores and $\mathrm{NE}\,\Delta T$ is the noise equivalent temperature difference (Hopper 1993). Radiometric temperature changes measured in each image ($\Delta M(x, y, t_0)$) were calibrated using a resistor-heated aluminium surface coated with highly emissive ($\varepsilon \approx 0.967$) black paint (TC-303 black, GIE-Tracor, Provo, UT) positioned in object space conjugate to the IR FPA. A surface mount thermistor (model No 8681, Keithley, Cleveland, OH) measured temperature (sensitivity $< 0.01\,^{\circ}\mathrm{C}$) as the surface was slowly heated ($1\,^{\circ}\mathrm{C\ min}^{-1}$).

An *in vitro* model using thin (i.e., 50–150 μm) collagen films (F1310, Collatec, Plainsboro, NJ) containing variable amounts of absorber was used to simulate discrete chromophores buried in multilayered composite human skin. Chromophores were

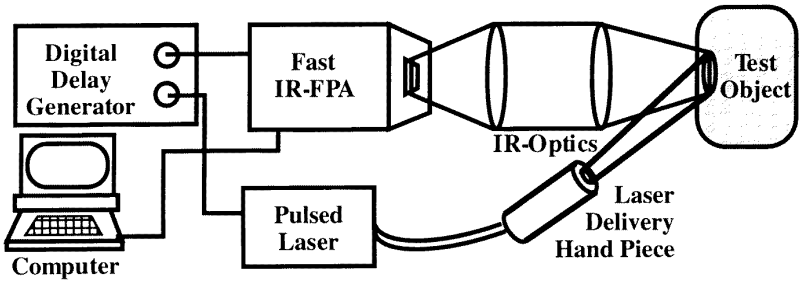

Figure 2. A schematic diagram of IRT instrumentation to measure the radiometric temperature change ($\Delta M(x, y, t_0)$).

constructed by staining a film with triphenylmethane dye (Aldrich Chemical Co., Milwaukee, WI) which absorbs optimally at the wavelength utilized in the experiments. Discrete chromophores were prepared by cutting a stained collagen film ($w_z = 125$ μm) with known optical absorbance ($\mu_a = 40$ mm^{-1}) into a number of thin strips ($w_x = 100$–300 μm). The linear orientation of the stained collagen strips used in our study was selected to simulate blood vessels present in multilayered human skin. A model skin phantom was constructed by positioning variably spaced (50–700 μm) phantom blood vessels underneath a known thickness of weakly absorbing collagen films. Phantom blood vessels and collagen films were positioned on a 10 mm thick collagen sponge to simulate an infinite half-space as in *in vivo* skin. Pulsed ($t_p = 0.45$ ms) radiation ($\lambda = 585$ nm) released from a flashlamp pumped dye laser (SPTL-1, Candela, Wayland, MA) was incident on the material at 30° from the surface normal and covered a 30 mm^2 elliptical area. Immediately following exposure to a 1.0–1.5 J laser pulse, a time sequence of 100–200 images of radiometric temperature ($M(x, y, t)$) was recorded by the IR FPA camera. The relationship between lateral resolution and chromophore depth was investigated by placing the stained collagen strips underneath a variable number of weakly absorbing collagen films of different thicknesses (110, 180, 280, 380 μm).

From each recorded time sequence of radiometric temperature ($M(x, y, t)$), the earliest time (t_0) was identified that gave images with greatest contrast. At each selected time, a given number of frames (217 (frames s^{-1}) $\times$ (t_0/10)s) centred about t_0 were averaged to give a mean radiometric temperature $\overline{M}(x, y, t_0)$. Representative times and corresponding number of frames for each model system tested (i.e., chromophores at depths of 110, 180, 280, 380 μm) were, respectively, 32, 69, 207, and 295 (ms) and one, one, four, and six frames. The mean radiometric temperature change at time $t_0(\overline{\Delta M}(x, y, t_0))$, was obtained by subtracting the non-irradiated background temperature and averaging over selected frames.

4. Results and discussion

The reduced two-dimensional temperature increase $\Delta T^{2D}(x, y, t_0)$ was computed (figure 3) for each model by applying the non-negative constrained conjugate gradient algorithm using $\overline{\Delta M}(x, y, t_0)$ as input data. Assumed values of thermal diffusivity, conductivity, and heat loss coefficient in all calculations were, respectively, 1.1×10^{-7} m^2 s^{-1}, 0.45 W mK^{-1}, and 15 W m^{-2} K^{-1} (Duck 1990). At deeper depths, lateral physical dimensions of subsurface chromophores determined by deconvolution increase because thermal diffusion strongly attenuates higher-order spatial frequencies required for fine spatial resolution.

Lateral physical dimensions are best resolved and closely match prepared values when chromophores are positioned closest to the surface (figure 3(A)). Individual closely spaced (50–100 μm) chromophores positioned deeper than 280 μm are more difficult to resolve (figure 3(C,D)). For example, at depths of 280 μm or deeper, resolution of three linear chromophores located in the upper leftmost region of the irradiation zone is not possible (figure 3(C)). A central pair of nearly parallel linear chromophores easily differentiated when irradiated at superficial positions is difficult to resolve when located at a depth of 380 μm (figure 3(D)).

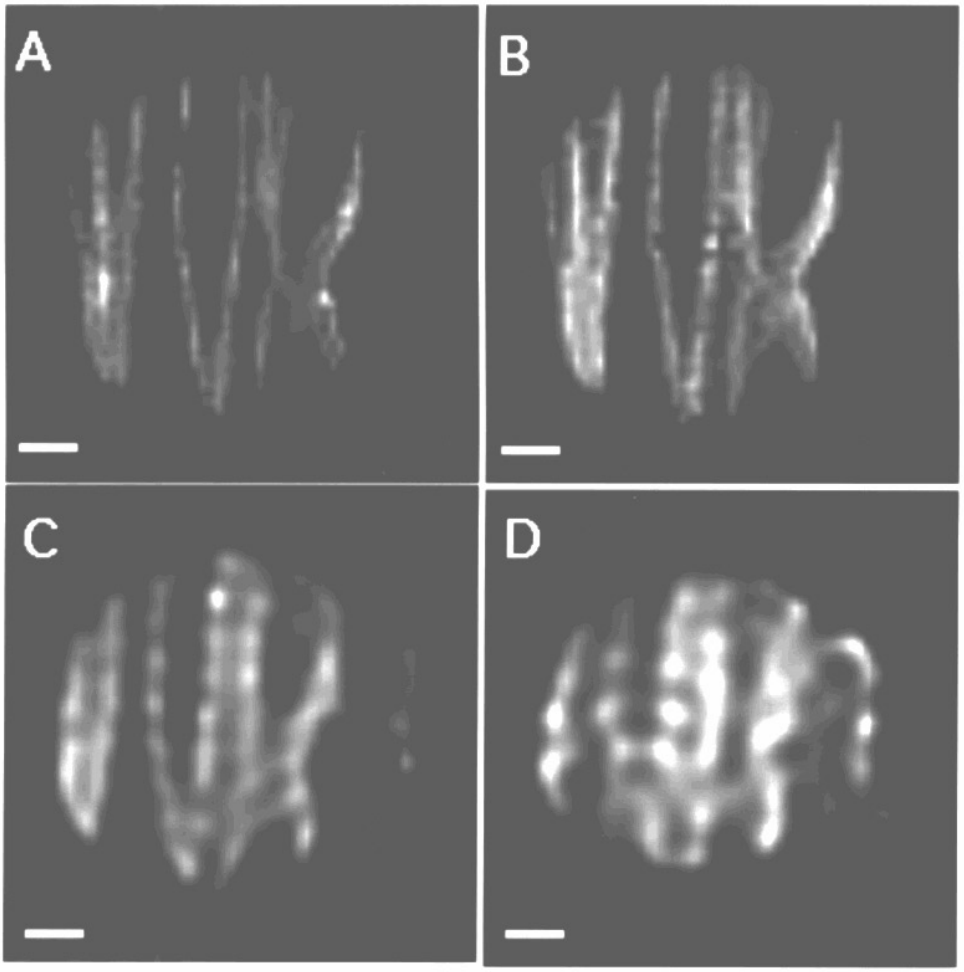

Figure 3. Deconvolved images of the reduced two-dimensional subsurface temperature increase ($\Delta T^{2D}(x, y, t_0)$) representing chromophores positioned at depths (z_0) of (A) 110 μm, (B) 180 μm, (C) 280 μm, and (D) 380 μm. (The bar represents 1 mm.)

4.1. Discussion of results

Reduction in spatial resolution when imaging deeper chromophores is due to decreased radiometric temperature changes that originate from increased lateral (K_r, (9*a*)) and longitudinal (K_z, (9*b*)) thermal diffusion. Although SNR can increase in later frames as heat moves from chromophores to the material surface, greater lateral thermal diffusion blurs images and limits spatial resolution. Increased SNR may be obtained by use of higher laser irradiance which would produce a larger initial temperature increase. Because protein denaturation can significantly change thermal properties of biological materials (Si *et al* 1995), however, caution should be exercised when using higher laser irradiance. In deriving (14), for example, we assumed that thermal properties are constant and homogeneous during and following pulsed laser irradiation. When protein denaturation due to excessive laser heating occurs, thermal diffusivity (χ) changes and, consequently, errors and artifacts are introduced into the analysis.

Instrumentation and conditions employed in preliminary experiments reported here were far from ideal. For example, the IR FPA suffered from time-dependent temperature fluctuations. Although IR FPA non-uniformities were corrected prior to experimentation using a standard two-point hot–cold calibration procedure, the time-dependent nature of the fluctuations reduced SNR. In the following analysis, use of an optimized IR FPA camera is assumed and we analyse effects of chromophore depth (z_0) and infrared absorption (μ_{ir}) on lateral spatial resolution.

4.2. The radiometric transfer function

A radiometric transfer function ($\Delta R(k, t, z_0)$) is derived that relates peak-to-peak amplitude of true radiometric temperature increase in response to uniform heating of a linear array of identical subsurface chromophores in a biological material (figure 1). Specifically, we assume a homogeneous 1 °C initial three-dimensional temperature increase ((18) below) in a uniform array of infinitely long linear chromophores positioned at depth z_0 of rectangular cross section $w_x \times w_z$ with centre-to-centre spacing Δx_0,

$$\Delta T^{3D}(x, y, z; t = 0) = \mathrm{rect}[(z - z_0)/w_z]\mathrm{rect}(x/w_x) * (1/\Delta x_0)\mathrm{comb}(x/\Delta x_0) \tag{18}$$

where rect(·) and comb(·) are standard notation for, respectively, rectangle and comb functions (Goodman 1985). From (10), and explicit expressions for lateral (K_r, (9*a*)) and longitudinal (K_z, (9*b*)) point spread functions, the peak-to-peak amplitude of the true radiometric temperature increase at the fundamental spatial frequency (k_0) is computed ($\Delta R(k_0 = 1/\Delta x_0, t, z_0)$, (19) below) by integrating $\Delta T^{3D}(x, y, z, t = 0)$ in an arbitrary (y, z) plane, followed by one-dimensional Fourier transformation along the x-axis (i.e., perpendicular to the long axis of each subsurface chromophore), and extraction of the k_0 harmonic.

$$\begin{aligned}\Delta R(k_0, t, z_0) = {} & w_x k_0 \mathrm{sinc}(w_x k_0) \mathrm{e}^{-\pi^2(2\sigma^2 + 4\chi t)k_0^2} \mathrm{e}^{-z^2/4\chi t} [\mathrm{erfcx}(u_+) - \mathrm{erfcx}(u_-) \\ & + [2/(h/\kappa - \mu_{ir})](\mu_{ir}\mathrm{erfcx}(u_1) - (h/\kappa)\mathrm{erfcx}(u_+)]\Big|_{z_0 - w_z/2}^{z_0 + w_z/2}\end{aligned} \tag{19}$$

where $\mathrm{sinc}(x) = \sin(\pi x)/(\pi x)$. We consider a spacing, Δx_0, between adjacent chromophores that is twice their lateral width (i.e., $\Delta x_0 = 2w_x$), so that $w_x k_0 \mathrm{sinc}(w_x k_0) = 1/\pi$. The peak-to-peak amplitude of the true radiometric temperature increase at the fundamental spatial frequency ($\Delta R(k_0, t, z_0)$) is a product of two terms that represent lateral and longitudinal heat diffusion. Inasmuch as optimum contrast is realized at a time t_0 when

the peak-to-peak amplitude of the true radiometric temperature increase is maximum, we compute $\partial[\Delta R(k_0, t, z_0)]/\partial t$.

$$\frac{\partial \Delta R(k_0, t, z_0)}{\partial t} = \chi(\mu_{ir}^2 - 4\pi^2 k_0^2)\Delta R(k_0, t, z_0) + 2\chi\mu_{ir}(\mu_{ir} + h/\kappa)P(t) \tag{20}$$

where

$$P(t) = \mathrm{e}^{-\pi^2(2\sigma^2+4\chi t)k_0^2}\mathrm{e}^{-z^2/4\chi t}\mathrm{erfcx}(u_1)\Big|_{z_0-w_z/2}^{z_0+w_z/2}.$$

Examination of $\partial[\Delta R(k_0, t, z_0)]/\partial t$ reveals a number of important observations directly relevant to the temporal evolution of $\Delta R(k_0, t, z_0)$. First, (20) may be viewed as a first-order differential equation for $\Delta R(k_0, t, z_0)$ in which the radiometric transfer function rate of increase is self-proportional plus an additional term, $2\chi\mu_{ir}(\mu_{ir} + h/\kappa)P(t)$. Second, for physically realistic values of h, representative of radiative and/or convective cooling (i.e., $h < 5$ kW m^{-2} K^{-1}), $P(t)$ is negative at all times, $t > 0$; at $t = 0$, $P(t) = 0$ and, thus, $\partial\Delta R(k_0, t = 0, z_0)/\partial t = \chi(\mu_{ir}^2 - 4\pi^2 k^2)\Delta R(k_0, t = 0, z_0)$. Third, since $\Delta R(k_0, t, z_0)$ is strictly positive for $t \geqslant 0$, $\chi(\mu_{ir}^2 - 4\pi^2 k^2) < 0$ gives $\partial\Delta R(k_0, t \geqslant 0, z_0)/\partial t < 0$ and thus $\Delta R(k_0, t, z_0)$ assumes a maximum value at $t_0 = 0$; conversely, when $\chi(\mu_{ir}^2 - 4\pi^2 k^2) > 0$, $\partial\Delta R(k_0, t, z_0)/\partial t \geqslant 0$ for some time interval $[0, t_0]$, and $\Delta R(k_0, t, z_0)$ assumes a maximum value at time $t_0 > 0$. At fine spatial frequencies (i.e., large k_0), reduction of peak-to-peak amplitude due to lateral blurring dominates over increases from longitudinal diffusion; in these cases, optimum contrast of laser heated subsurface chromophores is achieved at $t_0 = 0$. Source distributions at an equal depth with coarser spatial frequencies less than a characteristic value (i.e., $k_0 < \mu_{ir}/2\pi$) are blurred less and allow heat in subsurface chromophores to diffuse to the material surface giving optimum contrast at a later time ($t_0 > 0$). To illustrate these features, we plot (figure 4) the temporal dependence of the contrast ($\Delta R(k_0, t, z_0)$) representing subsurface linear chromophores at $z_0 = 300$ μm, with $\mu_{ir} = 30$ mm^{-1} and $h = 15$ W m^{-2} K^{-1} for three spatial frequencies. We observe, for $k_0 > \mu_{ir}/2\pi$, that optimum contrast is attained at $t_0 = 0$; alternatively, when $k_0 < \mu_{ir}/2\pi$ optimum contrast is found at time $t_0 > 0$. When $k_0 = \mu_{ir}/2\pi$, the slope of $\Delta R(k_0, t, z_0)$ at $t = 0$ is zero, consistent with (20).

We compute optimum contrast ($\Delta R(k_0, t_0, z_0)$) versus the fundamental spatial frequency (k_0) for a linear array of identical laser heated subsurface chromophores of square cross-section (i.e., $w_z = w_x$) positioned at various depths (z_0) with $\mu_{ir} = 30$ mm^{-1} and $h = 15$ W m^{-2} K^{-1}. When $\chi(\mu_{ir}^2 - 4\pi^2 k^2) > 0$, optimum contrast is found by numerical determination of time t_0 which satisfies $\partial[\Delta R(k_0, t_0, z_0)]/\partial t = 0$, and evaluation of $\Delta R(k_0, t_0, z_0)$; conversely, when $\chi(\mu_{ir}^2 - 4\pi^2 k^2) < 0$, the value of optimum contrast is $\Delta R(k_0, t_0 = 0, z_0)$ as discussed above. At any chromophore depth z_0, only spatial frequencies $k_0 \geqslant 1/4z_0$ are considered; when $k_0 = 1/4z_0$, the uppermost facet of each linear chromophore is coincident with the surface of the biological material. We compute (figure 5) the optimum contrast representative of a linear array of identical laser heated subsurface chromophores of square cross-section positioned at depths $z_0 = 100$ μm, 200 μm, 300 μm, and 400 μm. Optimum contrast decreases monotonically with increasing spatial frequency (k_0) for chromophores at any depth. The slope of $\Delta R(k_0, t_0, z_0)$ changes at $k_0 = \mu_{ir}/2\pi$: for $k_0 < \mu_{ir}/2\pi$, optimum contrast is limited by longitudinal diffusion and decays very rapidly for increasing spatial frequency; when $k_0 > \mu_{ir}/2\pi$, lateral diffusion dominates and the optimum contrast decreases less rapidly for increasing spatial frequency. At any spatial frequency (k_0), optimum contrast rapidly decreases with deeper chromophore depths (z_0).

Optimum contrast is also dependent on the infrared absorption coefficient (μ_{ir}). We assume a linear array of infinitely long chromophores of square cross-section positioned

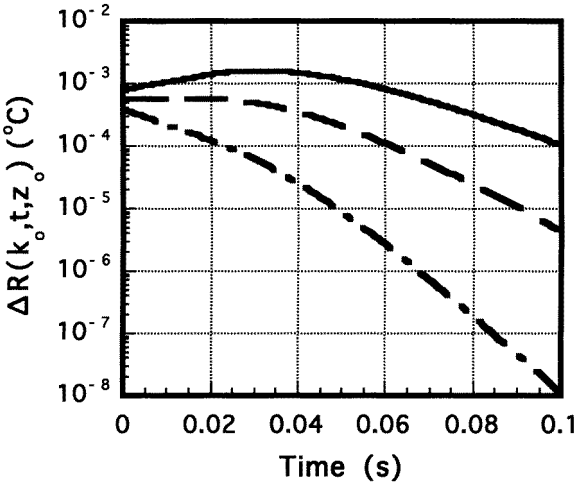

Figure 4. The temporal dependence of the contrast ($\Delta R(k_0, t, z_0)$) for a uniform linear array of chromophores ($z_0 = 300$ μm, $\mu_{ir} = 30$ mm^{-1}, and $h = 15$ W m^{-2} K^{-1}) at three spatial frequencies: $k_0 < \mu_{ir}/2\pi$ (——); $k_0 = \mu_{ir}/2\pi$ (– – –); and $k_0 > \mu_{ir}/2\pi$ (— · —).

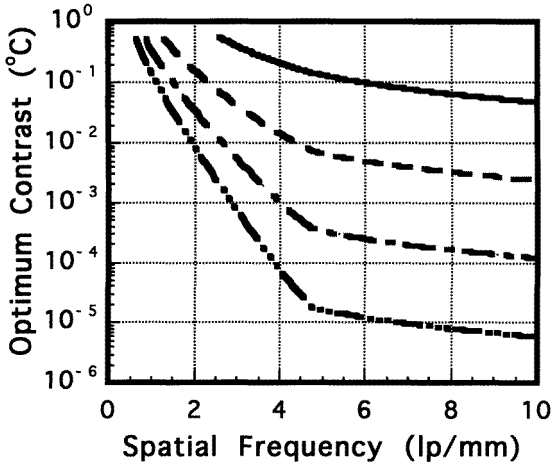

Figure 5. The optimum contrast ($\Delta R(k_0, t_0, z_0)$) representative of a uniform linear array of chromophores positioned at depths (z_0) of 100 μm (——), 200 μm (– – –), 300 μm (— · —), and 400 μm (—· ·—), with $\mu_{ir} = 30$ mm^{-1} and $h = 15$ W m^{-2} K^{-1}.

at depth $z_0 = 250$ μm with surface heat loss coefficient $h = 15$ W m^{-2} K^{-1} representative of radiative and natural convective energy losses and compute optimum contrast ($\Delta R(k_0, t_0, z_0)$, figure 6) for $\mu_{ir} = 10$, 25, and 50 mm^{-1}. At greater μ_{ir}, a change of slope, indicative of the transition from longitudinal- to lateral-dominated diffusive blurring ($k_0 = \mu_{ir}/2\pi$), moves to finer (higher) spatial frequencies. At these spatial frequencies (e.g., $k_0 > 8$ mm^{-1}), the optimum contrast is strongly dependent on the magnitude of μ_{ir}; an increase of μ_{ir} from 10 mm^{-1} to 50 mm^{-1} decreases $\Delta R(k_0, t_0, z_0)$ by more than 60 dB.

The magnitude of μ_{ir} is a spectral- and temperature-dependent function (i.e., $\mu_{ir} = \mu_{ir}(\lambda, T)$) of each molecular species present in the laser-irradiated material. Primary

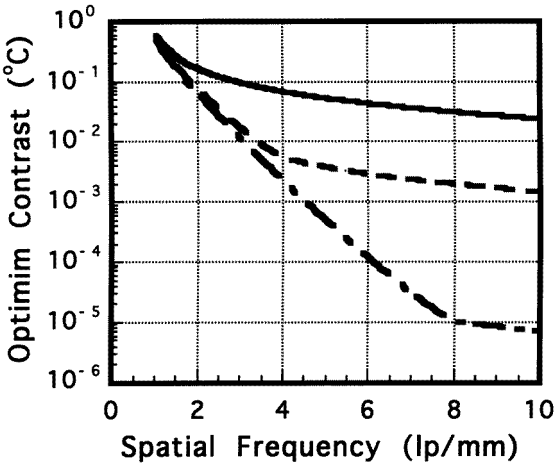

Figure 6. The optimum contrast ($\Delta R(k_0, t_0, z_0)$) of a uniform linear array of chromophores positioned at a depth $z_0 = 250$ μm in a biological material with infrared absorption coefficient $\mu_{ir} = 10$ mm^{-1} (——), 25 mm^{-1} (- - - -), and 50 mm^{-1} (— · —).

constituents in mammalian tissue are collagen and water; for example, in human dermis, water and collagen comprise, respectively, approximately 70% and 30% of *in vivo* mass (von Zglinicki *et al* 1993). The infrared absorption coefficient of collagen (Doyle and Blout 1975) lies in a relative local minimum between amide I and amide A–B absorption peaks approximately centred at, respectively, $\lambda = 3.1$ and 6.0 μm (Arrondo *et al* 1993). Similarly, the infrared absorption coefficient of water ($\mu_{ir}(H_2O)$) also falls to minimum values between two absorption peaks approximately centred at $\lambda = 2.9$ and 6.6 μm (Hale and Querry 1973, Wieliczka *et al* 1989). At physiological temperatures ($\sim 33\,^{\circ}$C), $\mu_{ir}(H_2O)$ varies over 10–40 mm^{-1} in the 4–5.4 μm spectral region and can decrease at least twofold for a moderate increase of 40 °C (Marechal 1991).

If we assume a uniform temperature increase $\Delta T^{3D}(x, y, z, t = 0) \approx 30\,^{\circ}$C) in an infinite linear array of square chromophores ($w_x = w_z = 50$ μm, $k_0 = 10$ mm^{-1}) positioned at a depth of $z_0 = 250$ μm with $\mu_{ir} = 10$ mm^{-1}, then the optimum contrast is $\Delta R(k_0, t_0 = 0, z_0) = 0.6\,^{\circ}$C (figure 6). At a 120 Hz frame rate, use of a commercially available IR FPA camera that is detector noise limited allows NE$\Delta T < 0.01\,^{\circ}$C (Wilson *et al* 1992) or equivalent SNR ≈ 60. We conclude, therefore, that if μ_{ir} is sufficiently small, use of an optimized IR FPA camera in combination with deconvolution of the derived imaging equation may provide a useful means to determine lateral physical dimensions of subsurface chromophores in human skin. Experiments that measure μ_{ir} of human skin at various temperatures in the infrared spectral region are under way in our laboratory.

5. Conclusions

We have derived an imaging equation that relates the measured radiometric temperature change of a laser irradiated biological material to the reduced two-dimensional temperature increase of subsurface chromophores. Estimation of lateral physical dimensions of chromophores requires deconvolution of the derived imaging equation to determine the reduced two-dimensional temperature increase. Measurements of the radiometric temperature change in response to pulsed laser irradiation of an *in vitro* collagen model of

multilayered composite human skin are applied to determine the reduced two-dimensional temperature increase and thus estimate lateral physical dimensions of prepared subsurface chromophores. Deconvolution of the derived imaging equation by an efficient non-negative constrained conjugate gradient algorithm indicates that spatial resolution rapidly degrades with increasing chromophore depth due to longitudinal and lateral heat diffusion. Derivation of a radiometric transfer function predicts that for increasing spatial frequencies a transition from longitudinal- to lateral-dominated diffusive blurring occurs when $k_0 = \mu_{ir}/2\pi$. Decay of optimum contrast for increasing spatial frequency is most rapid when blurring is dominated by longitudinal thermal diffusion. Sufficient contrast (SNR = 60) of small-diameter (50 μm) subsurface chromophores (250 μm deep) such as port wine stain blood vessels in human skin heated by a diagnostic laser pulse (i.e., < 2.5 J cm^{-2}) may be possible if μ_{ir} is sufficiently small ($\mu_{ir} \sim 10$ mm^{-1}).

Acknowledgments

This project was supported by research grants awarded from the Biomedical Research Technology Program (R03-RR06988) and Institute of Arthritis and Musculoskeletal and Skin Diseases (1R29-AR41638-01A1 and 1R01-AR42437-01A1) at the National Institutes of Health, Whitaker Foundation, and Dermatology Foundation to JSN. Institutional support from the Office of Naval Research, Department of Energy, National Institutes of Health, and the Beckman Laser Institute and Medical Clinic Endowment is also gratefully acknowledged. Work of Dennis Goodman performed under the auspices of the US Department of Energy by the Lawrence Livermore National Laboratory under contract W-7405-Eng-48. The work of B S Tanenbaum was supported in part by the National Institutes of Health (grant R-15-AR43403-01) and by a Whitaker Foundation Special Opportunity Award. Sun Microsystems Computing Corporation provided the resources necessary to complete the computations. The Office of Academic Computing at the University of California, Irvine, provided indispensable technical assistance. Chris Johnston of Amber Engineering generously provided the use of the IR FPA camera system.

References

Anderson R R and Parish J A 1983 Selective photothermolysis: precise microsurgery by selective absorption of pulsed radiation *Science* **220** 524–7

Arrondo J L R, Muga A, Castresana J and Goñi F M 1993 Quantitative studies of the structure of proteins in solution by Fourier-transform spectroscopy *Prog. Biophys. Mol. Biol.* **59** 23–56

Doyle B B and Blout E R 1975 Infrared spectroscopy of collagen and collagen-like peptides *Biopolymers* **14** 937–57

Duck F A 1990 *Physical Properties of Tissue. A Comprehensive Reference Book* (London: Academic)

Goodman D M, Johansson E and Lawrence T E 1992 On applying the conjugate gradient method to image processing problems *Multivariate Analysis: Future Directions* ed C R Rao (Amsterdam: North-Holland)

Goodman J W 1968 *Introduction to Fourier Optics* (San Francisco: McGraw-Hill)

——1985 *Statistical Optics* (New York: Wiley)

Hale G M and Querry M R 1973 Optical constants of water in the 200-nm to 200-mm wavelength region *Appl. Opt.* **12** 555–63

Hopper G S 1993 Forward looking infrared systems *Passive Electro-Optical Systems* ed S B Campana (Ann Arbor, Bellingham, WA: ERIM–SPIE)

Ishimaru A 1978 *Wave Propagation and Scattering in Random Media* (New York: Academic)

Kimel S, Svaasand L O, Wilson M H, Schell M J, Milner T E, Nelson J S and Berns M W 1993 Differential vascular response to laser photothermolysis *J. Invest. Dermatol.* **103** 693–700

Marechal Y 1991 Infrared spectra of water I. Effect of temperature and of H/D isotopic dilution *J. Chem. Phys.* **95** 5565–73

McCormick G P 1969 Anti-zigzagging by bending *Management Sci.* **15** 315–9

Milner T E, Goodman D M, Tanenbaum B S and Nelson J S 1995 Depth profiling of laser-heated chromophores in biological tissues by pulsed photothermal radiometry *J. Opt. Soc. Am.* A **12** 1479–88

Prahl S A, Vitkin I A, Bruggemann U, Wilson B C and Anderson R R 1992 Determination of optical properties of turbid media using pulsed photothermal radiometry *Phys. Med. Biol.* **37** 1203–17

Si M S, Milner T E, Anvari B and Nelson J S 1995 Dynamic heat capacity changes of laser irradiated type I collagen films *Lasers Surg. Med.* at press

Tam A C 1987 Pulsed laser photoacoustic and photothermal detection *Photoacoustic and Thermal Wave Phenomena in Semiconductors* ed A Mandelis (New York: North-Holland) pp 175–200

van Gemert M J C, Welch A J, Miller I D and Tan O T 1991 Can physical modeling lead to an optimal laser treatment strategy for port wine stains? *Laser Applications in Medicine and Biology* ed M Wolbarsht (New York: Plenum)

Vitkin I A, Wilson B C and Anderson R R 1995 Analysis of layered scattering materials by pulsed photothermal radiometry: application to photon propagation in tissue *Appl. Opt.* **34** 2973–82

von Zglinicki T, Lindberg M, Roomans G M and Forslind B 1993 Water and ion distribution profiles in human skin *Acta Dermatol. Venereol.* **73** 340–3

Wieliczka D M, Weng S and Querry M R 1989 Wedge shaped cell for highly absorbent liquids: infrared optical constants of water *Appl. Opt.* **28** 1714–9

Wilson T E, Henricks T F, Halvis J and Rosner B D 1992 Versatile multi mode $320 \times 240/256 \times 256$ hybrid InSb infrared focal plane array with selectable snapshot or rolling integration *Proc. SPIE* **1762** 401–6